Turkish Journal of Electrical Engineering & Computer Sciences

http://journals.tubitak.gov.tr/elektrik/

Research Article

Turk J Elec Eng & Comp Sci
(2017) 25: 1412 – 1425

doi:10.3906/elk-1602-381

Design and operation of a multifunction photovoltaic power system with shunt active filtering using a single-stage three-phase multilevel inverter

Serkan SEZEN[1], **Ahmet AKTAŞ**[2], **Mehmet UÇAR**[3], **Engin ÖZDEMİR**[2,*]
[1]Edremit Vocational School, Balıkesir University, Balıkesir, Turkey
[2]Department of Energy Systems Engineering, Faculty of Technology, Kocaeli University, Kocaeli, Turkey
[3]Department of Electrical and Electronics Engineering, Faculty of Engineering, Düzce University, Düzce, Turkey

Received: 29.02.2016 • **Accepted/Published Online:** 11.05.2016 • **Final Version:** 10.04.2017

Abstract: In this paper, the control of a multifunction grid-connected photovoltaic (PV) system with a three-phase three-level (3L) neutral point clamped (NPC) inverter is proposed, which can perform shunt active filtering. Normally, the shunt active filtering is achieved by detecting the harmonic and reactive currents of the nonlinear load and then injecting the compensating current into the grid. Therefore, the proposed system can inject PV power to a grid with power factor correction and current harmonic filtering features simultaneously. In addition, a single-stage compact and efficient transformerless power conversion topology is used in this paper for the grid-connected solar PV system with maximum power point tracking capability. In order to control the multilevel inverter-based combined system, a synchronous reference frame control technique and hysteresis current control pulse width modulation method have been applied. The system configuration and control strategy are verified and validated by simulations based on MATLAB/Simulink and implemented in real-time using the dSPACE DS1103 controller board. The simulation with experimental results indicates that the injected currents are sinusoidal and current total harmonic distortion is about 3.9%, lower than the IEEE 519 harmonic limit.

Key words: Active filter, harmonic distortion, multilevel inverter, photovoltaic power system, reactive power

1. Introduction

Nowadays, one of the most popular forms of renewable energy is solar energy. Solar photovoltaic (PV) systems range from several tens of kilowatts to hundreds of megawatts. Recently, most PV systems are grid-connected, while stand-alone systems only account for a small portion of the power market [1–4]. PV grid-connected systems have the benefit of more efficient usage of power generation because there are no additional battery storage losses. The designing of the PV systems that can maximize energy production from the sun through solar PV modules is an important factor. Maximum power point tracking (MPPT) techniques are widely used to maximize the power output of the solar PV module. Several MPPT techniques were proposed in the literature, such as the constant voltage method, constant current method, short-circuit current method, open voltage method, perturb and observe (P&O) method, incremental conductance method, and temperature method [5–7]. The P&O MPPT method is commonly used because of its easy implementation [5]. There are different power circuit topologies and control methods used in grid-connected PV systems in the literature [8–11].

High-power equipment limits the maximum DC-bus voltage level because of the high voltage requirement

*Correspondence: eozdemir@kocaeli.edu.tr

in PV power systems. Multilevel inverters are more effective than traditional two-level (2L) inverters due to their lower switching loss and transformer loss, even though more power devices are connected to the grid. The three-level (3L) inverter has better performance than 2L inverters in output power quality although it has lower switching frequency. The neutral point clamped (NPC) multilevel topology is more popular as it has some advantages: decreased switching losses, less output current ripple content, and shared total DC source voltage [12,13].

Nonlinear loads and power electronic devices are causes of harmonic voltage and current components in electric power systems. Thus, a solar PV power generation system including a shunt active filtering function connected to the grid would be very useful for the improvement of power quality for both costumers and utility operators [14–23]. The shunt active filtering functionality can be achieved only by changing the control algorithm of the inverter. It is recommended that inverters should be connected to the grid for improving the efficiency, reliability, and flexibility of PV power systems [24,25].

In this paper, the analysis, simulation, and experimental verification of a single-stage three-phase 3L NPC-based PV power system with shunt active filtering capability are presented. Figure 1 depicts the schematic diagram of the multifunction grid-connected PV system adopted in this work. In order to produce the compensation current references for shunt active filtering, the synchronous reference frame (SRF)-based control algorithm is used. Switching signals of the multilevel inverter are generated by the hysteresis current control (HCC) pulse width modulation (PWM) method. The P&O MPPT algorithm is used for improving the effectiveness of the proposed system. The overall performance of the proposed system is confirmed by simulations in MATLAB/Simulink and the dSPACE DS1103-based real-time controller board in the experiments. The obtained simulation and experimental results demonstrate the control and dynamic performance of the multifunctional grid-connected PV system with active filtering capability.

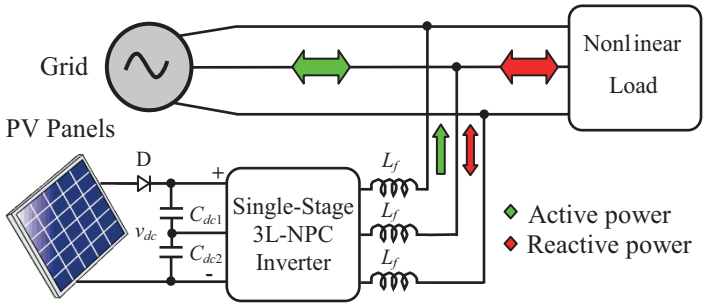

Figure 1. The schematic diagram of the multifunction grid-connected PV system.

2. Control of multifunction PV system with shunt active filtering

Inverter topologies and control strategies of the shunt active filtering and grid-connected PV systems are similar. If there is enough radiation during the day, the combined PV system is able to supply active power to the grid as well as compensate the current harmonics. In this work, a DC-DC converter is not required because MPPT operates in integration with the DC-bus controller. Figure 2 shows the control block diagram of the single-stage three-phase 3L-NPC inverter-based PV power system with shunt active filtering function.

In the proposed system controller, the active current reference (i_d^*) has two components as shown in Eq. (2). The first component, $i_{d\_vdc}^*$, indicates the amount of active power transferred to the network. This component is determined by the PI controller that compares the reference DC voltage generated by the MPPT

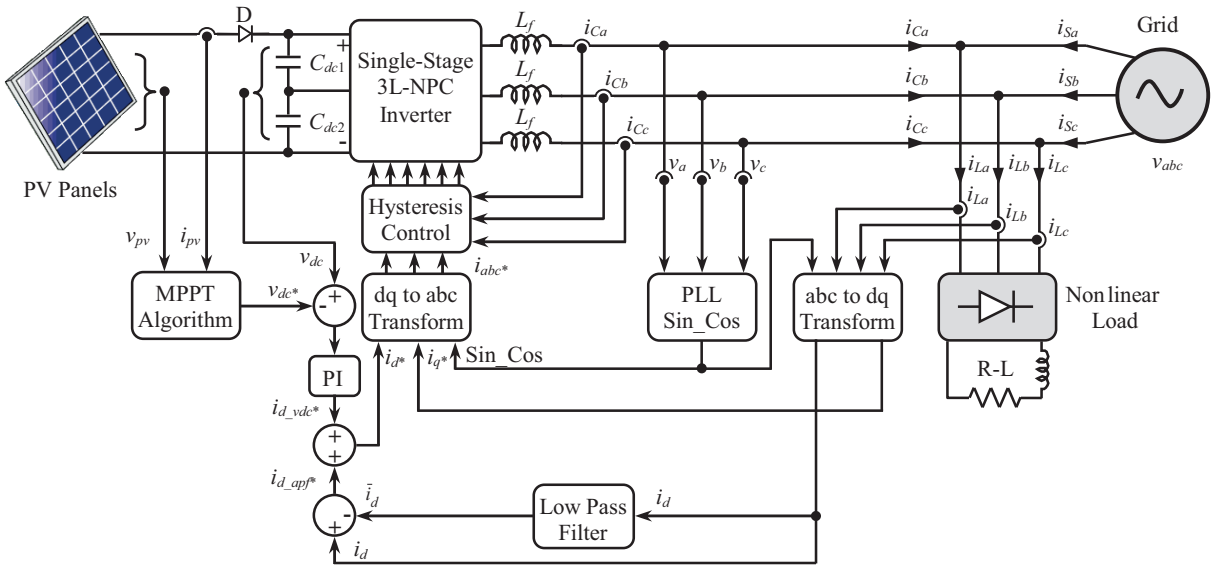

Figure 2. Control block diagram of PV power system with shunt active filtering function.

method and the measured DC-bus voltage (V_{dc}). The proposed MPPT algorithm's MATLAB/Simulink block diagram used in the PV power system is given in Figure 3. As shown in Figure 3, the measured voltage and current values are sampled and applied to the P&O MPPT control algorithm. Thus, the reference DC-bus voltage (V^*_{dc}) is obtained. The other component of the active current reference ($i^*_{d\_apf}$) generates the reference current signals for shunt active filtering. In order to generate this signal, measured load voltages are transformed to synchronous dq coordinates as in Eq. (1) at first, and then the d-axis load current component is passed from the low-pass filter to obtain the sine fundamental component without including harmonics. Finally, the $i^*_{d\_apf}$ component is obtained by subtracting the sine fundamental component from containing the harmonic component.

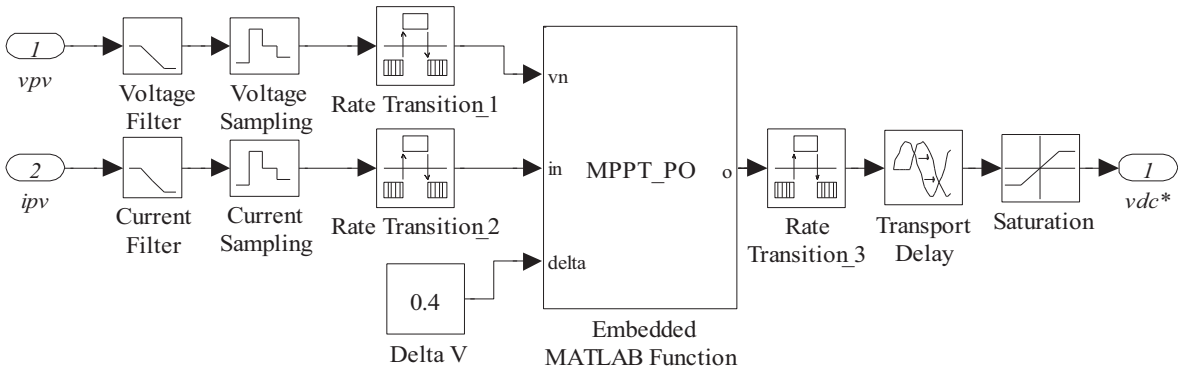

Figure 3. MATLAB/Simulink block diagram of the P&O MPPT controller.

$$\begin{bmatrix} i_d \\ i_q \end{bmatrix} = \frac{2}{3} \begin{bmatrix} \sin(\omega t) & \sin(\omega t - \frac{2\pi}{3}) & \sin(\omega t + \frac{2\pi}{3}) \\ cos(\omega t) & cos(\omega t - \frac{2\pi}{3}) & cos(\omega t + \frac{2\pi}{3}) \end{bmatrix} \begin{bmatrix} i_a \\ i_b \\ i_c \end{bmatrix} \tag{1}$$

$$i^*_d = i^*_{d\_vdc} + i^*_{d\_apf} \tag{2}$$

The resulting d-axis active current reference (i_d^*) and q-axis current reference (i_q^*) are subjected to the inverse dq transform process as in Eq. (3) in order to obtain the actual current references. These signals are then sent to the HCC for producing the switching signals [26,27].

$$\begin{bmatrix} i_a^* \\ i_b^* \\ i_c^* \end{bmatrix} = \begin{bmatrix} \sin(\omega t) & cos(\omega t) \\ \sin(\omega t - \frac{2\pi}{3}) & cos(\omega t - \frac{2\pi}{3}) \\ \sin(\omega t + \frac{2\pi}{3}) & cos(\omega t + \frac{2\pi}{3}) \end{bmatrix} \begin{bmatrix} i_d^* \\ i_q^* \end{bmatrix} \tag{3}$$

The MATLAB/Simulink block diagram of the HCC PWM for the 3L-NPC inverter-based proposed system is given in Figure 4. In the 3L-NPC inverter, there are three possible phase output voltage levels: $V_{dc}/2$, 0 (zero), and $-V_{dc}/2$. Accordingly, in order to reduce the actual current, one of two possible outputs (0, $-V_{dc}/2$) must be selected. Similarly, to increase the actual current, one of two possible outputs ($V_{dc}/2$, 0) must be selected. These selections are made by the 'Voltage Level Selection' block displayed in Figure 4 and switching signals are transferred to the output according to the selections. The preliminary results of this work were presented in a PEMC 2014 conference paper [28]. This paper presents the detailed design and operation of the proposed topology and MPPT controller algorithm including simulation and experimental results.

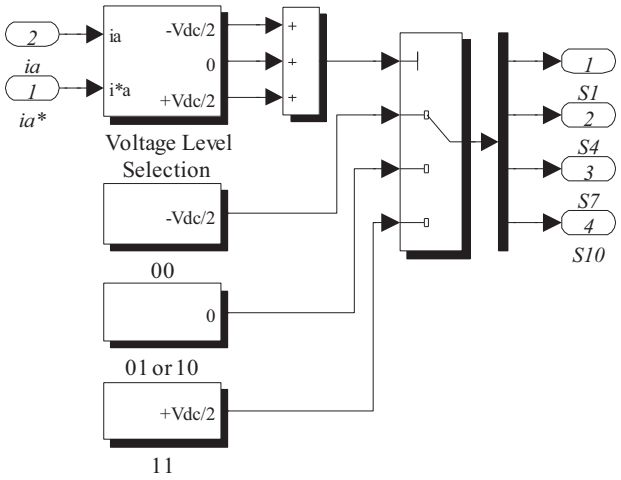

Figure 4. MATLAB/Simulink block diagram of the HCC PWM.

3. Simulation results

The feasibility of the proposed multifunction grid-connected PV system with shunt active filtering is proven by MATLAB/Simulink simulations. The three-phase full-wave rectifier with RL load is considered as a nonlinear load that injects harmonic currents and reactive power as well. The design parameters are listed in the Table for the proposed system. The proposed system performance has been analyzed in different operational modes. In the first mode, only the PV system power is transferred to the grid. In the second mode, the PV power system acts as a shunt active power filter. Thus, the proposed multilevel inverter can fulfill active power injection and active filtering functions simultaneously. In this work, the proposed system is simulated as only a grid-connected PV system in the first second and as a PV system with shunt active filtering functionality in the last second.

Table. Design parameters.

Grid	Voltage,v_{Sabc}	110 V_{rms}/L-N
	Frequency, f_S	50 Hz
Chroma PV simulator	Peak power, P_M Open circuit voltage, V_{OC} Short circuit current, I_{SC} Voltage at MPP, V_{MPP} Current at MPP, I_{MPP}	2000 Wp 457.8 V 5.75 A 370.5 V 5.40 A
PV system with shunt active filtering	DC-link voltage, V_{dc} Filter inductor,L_f DC-link capacitors, C_{dc1}, C_{dc2}	370 V 6.7 mH 2200 μF
Diode bridge rectifier load	Nonlinear load power, P_L DC side resistor-inductor, R_{dc}, L_{dc}	0.74 kW 90 Ω, 5.6 mH

In the simulation results, which are grid voltages and currents, multilevel inverter currents and nonlinear load currents are illustrated in Figures 5a–5d. The grid current waveforms are distorted with the only-PV system, while these waveforms are much closer to the sinusoidal waveform after shunt active filtering as shown in Figure 5b. The 3L-NPC inverter current waveforms are sinusoidal with the only-PV system, while these current waveforms include distortion of nonlinear load as shown in Figure 5c. The measured grid and inverter

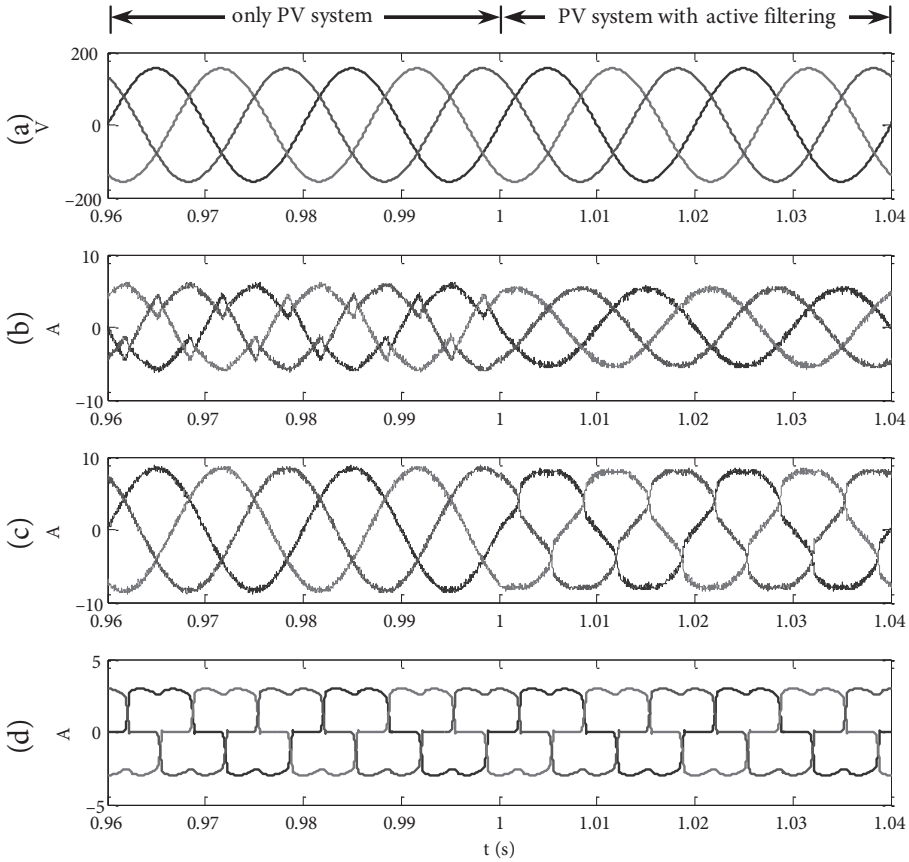

Figure 5. (a) Grid voltages, (b) grid currents, (c) inverter currents, and (d) load current waveforms.

output currents' total harmonic distortion (THD) values are indicated in Figure 6. The THD values of grid currents are close to the IEEE 519 harmonic limit value of 5% after shunt active filtering, as in this figure. In addition, Figure 7 demonstrates the MPPT voltage reference signal, 3L-NPC inverter DC-link voltage, and solar PV side power and current waveforms. In this figure, the DC-link voltage of the 3L-NPC inverter is very close to the MPPT output reference voltage. The current and power from the PV panel are maintained constant at the MPP under 1000 W/m^2 solar irradiance. It can be seen that the simulation results depict the proposed system to be more effective for solar PV real power injection, harmonic currents filtering, and reactive power compensation.

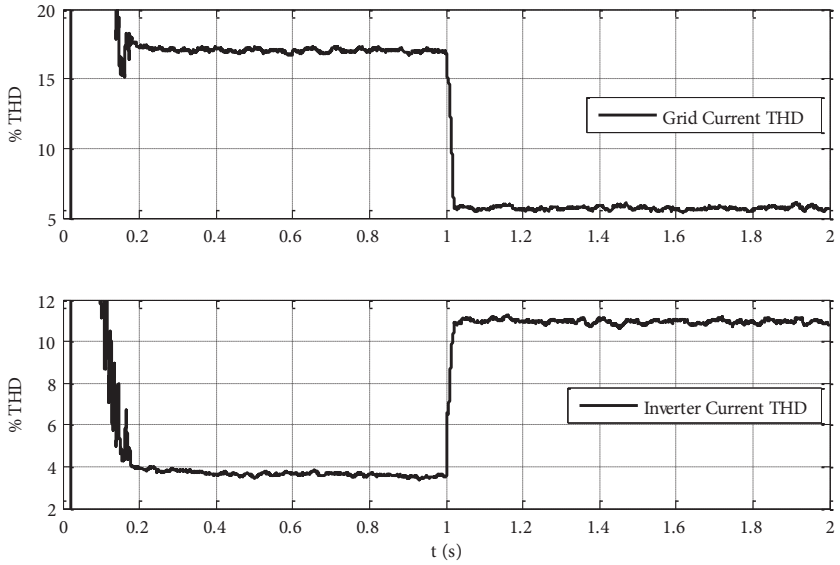

Figure 6. Grid current and inverter current THD waveforms.

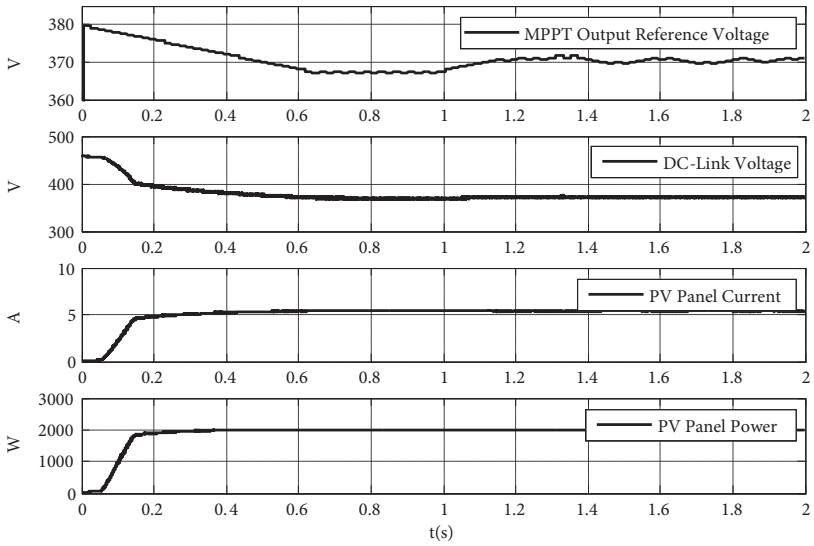

Figure 7. MPPT output reference voltage, DC-link voltage, PV power, and current waveforms.

4. Experimental results

The experimental setup was designed and implemented in the laboratory to prove its functionality. The controller was designed using a dSPACE DS1103 controller board. In the experimental study, the control block diagram was created in MATLAB/Simulink and then the generated C-code was directly downloaded to the dSPACE real-time control platform. The controller parameters can be adjusted interactively in the dSPACE Control Desk environment for improving system performance [29].

In the experimental setup, current and voltage values are measured with Hall effect-based TEG NA50-P current and TEG NV25-P voltage sensors. The DC-bus voltage is sensed with the AD210 three-port isolation amplifier. The obtained signals from the sensors are calibrated by using the signal conditioning interface boards and then applied to the dSPACE analog-to-digital converters (ADC) unit. In this paper, the sampling time for the control algorithm is set to 17 μs by using the dSPACE DS1103 board. The produced switching signals for the 3L-NPC inverter-based proposed PV system are taken via digital output channels of the dSPACE hardware. The experimental prototype power stage is composed of three Semikron SEMITOP SK50MLI060 dual-pack 3L NPC IGBT modules and six CT-CONCEPT 2SC0108T 2-channel gate driver boards. The measured 3L-NPC inverter currents are also used in the overcurrent protection board. The protection board is designed for the overcurrent and DC-bus overvoltage in the proposed system. If an error occurs, it disables the IGBT gate driver boards for power stage protection [29].

The experimental prototype of the multifunctional PV power system with active filtering capacity block diagram based on the 3L-NPC inverter is shown in Figure 8. The PV power system supplies three-phase sinusoidal currents for active power injection to the grid in only the grid-connected PV system mode. Nonlinear load current harmonic contents have been compensated from the grid, and thus the grid currents have a sinusoidal waveform in the active filtering function mode of the PV power system. In experimental studies, the Fluke 434 power quality analyzer was used to record the harmonic spectrum and a Tektronix DPO3054 digital oscilloscope was used to capture the waveforms. The experimental setup photograph is given in Figure 9. In this experimental study, a Chroma PV simulator 62050H-600S power supply is connected to the system to emulate the PV modules. The equipment can emulate the PV module characteristics under different irradiation conditions. In this paper, the PV simulator irradiation value is adjusted to 1000 W/m^2. The PV characteristic curves and operating points can be graphically monitored using a direct link between the PV simulator and connected PC. Figure 10 shows the Chroma PV simulator set to 2 kW and the control window used in the experimental tests.

The experimental results for the only grid-connected PV power system mode are illustrated in Figure 11 with waveforms of phase-a grid voltage (v_a) and current (i_{Sa}), 3L-NPC inverter (i_{Ca}), and load currents (i_{La}) correspondingly. In this case, the PV power is greater than the nonlinear load power and therefore the nonlinear load is fed by the PV power system and the remaining power is injected to the grid. While the inverter currents are sinusoidal, the grid currents have harmonics. The transient response of only the PV power system and with the shunt active filtering function is illustrated in Figure 12 with the voltage and current of the grid and inverter and load current for phase-a. It can be observed that the proposed system is initially operated in the PV system-only mode and feeds the PV power to the grid. The system finally switches to the PV system with shunt active filtering mode that compensates load harmonic currents and injects PV real power as well. In this study, the power factor control capability of the proposed system has been tested. The grid voltage and the grid current waveforms for phase-a without the PV system and for the PV system with and without shunt active filtering function are illustrated in Figures 13a–13c, respectively. As shown in Figure 13c, both grid voltage and grid current are in phase at near-unity power factor.

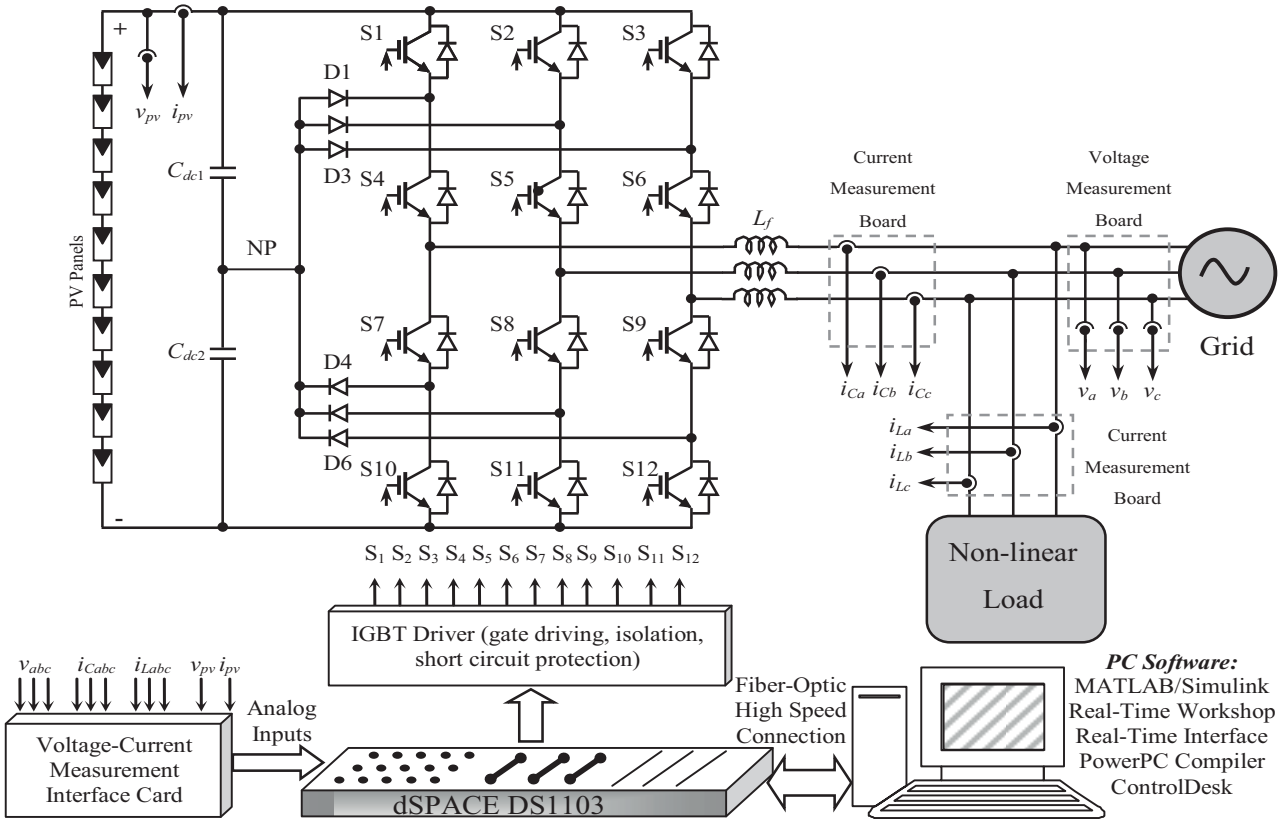

Figure 8. The experimental block diagram of the PV system with shunt active filtering.

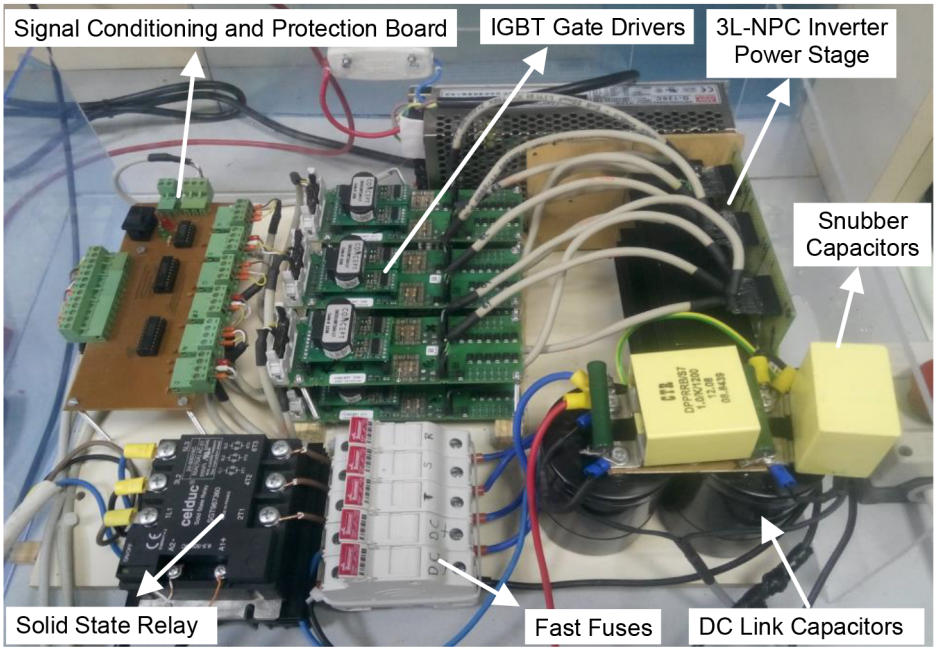

Figure 9. The experimental setup photograph.

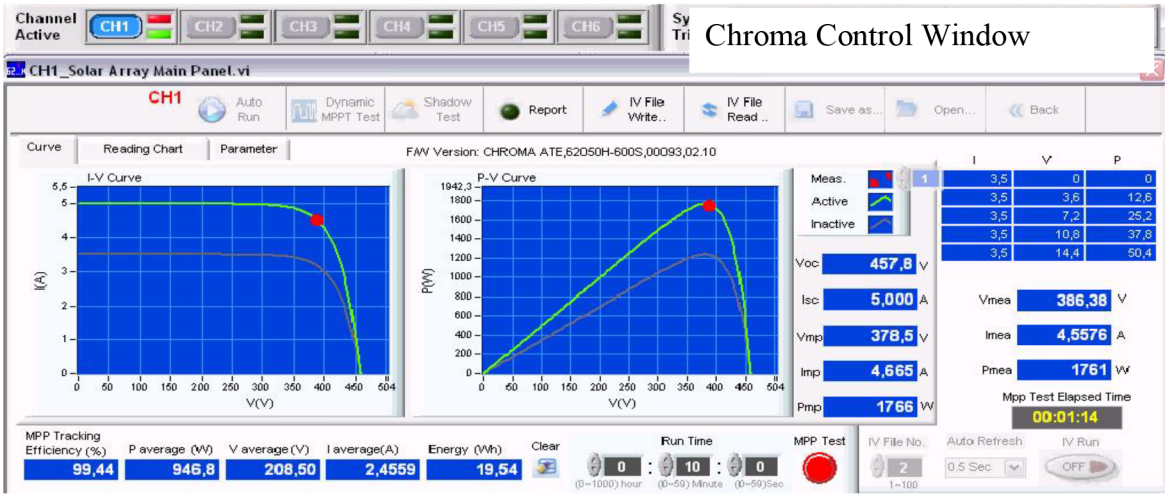

Figure 10. Chroma PV simulator control window.

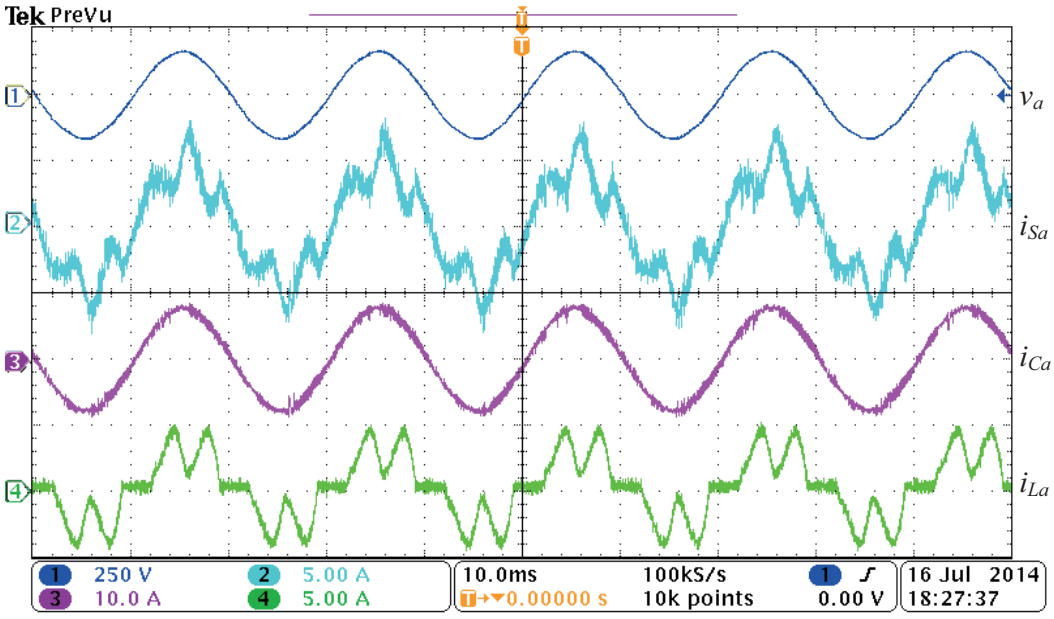

Figure 11. The experimental results for only grid-connected PV system mode.

The grid and inverter-side electrical parameters of the only grid-connected PV power system mode under 1000 W/m^2 solar irradiance are shown in Figure 14. The 2022 W DC power produced by PV panels is fed to the 3L-NPC inverter while 1950 W AC power is gained from the inverter output, 740 W of this power is used by the load, and the remaining 1210 W is supplied to the grid. In the mode without the active filtering function, nonlinear load current THD is 52.1%, grid current THD is 34.6%, and 3L-NPC inverter current THD is 2.3%.

The grid and inverter-side electrical parameters of the PV system with shunt active filtering mode under 1000 W/m^2 solar irradiance are shown in Figure 15. In the mode with the active filtering function, nonlinear load current THD is 52.1%, grid current THD is 3.9%, and 3L-NPC inverter current THD is 18.2%. The power

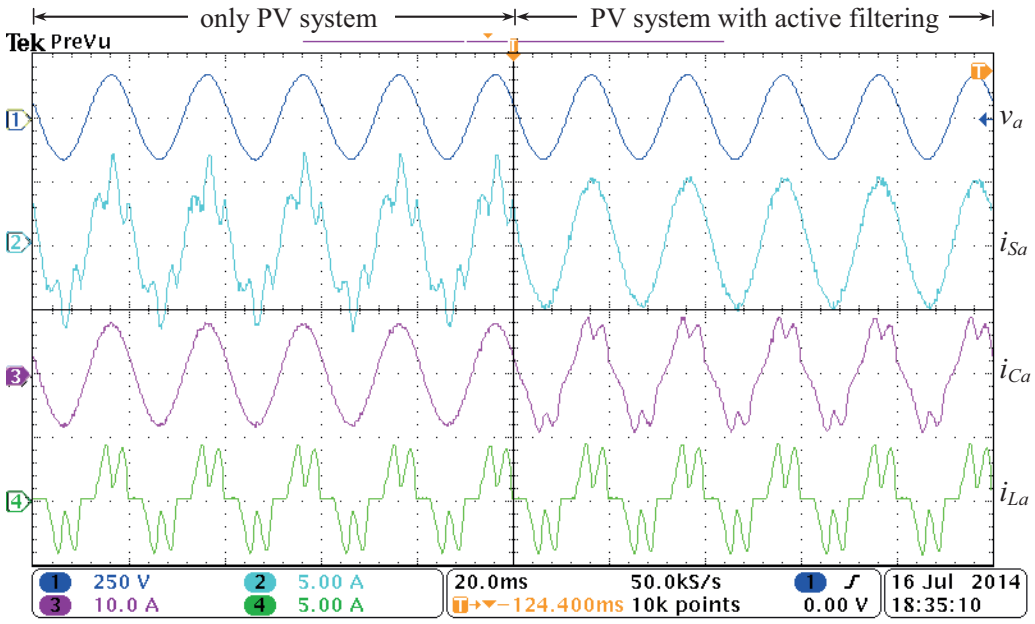

Figure 12. The transient response of the PV system with and without shunt active filtering.

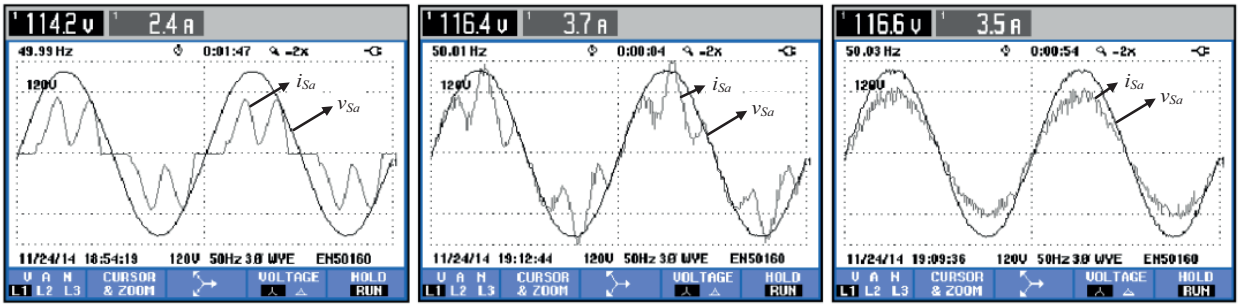

(a) (b) (c)

Figure 13. The grid voltage and current waveforms for phase-a: (a) without PV system, (b) only PV system, and (c) PV system with shunt active filtering.

factor (PF) of the grid side is 0.99 while that of the nonlinear load side is 0.87. Thus, a near-unity PF value is obtained.

In the experimental results for the PV system with active filtering condition, as the produced PV power is larger than the nonlinear load power, the 3L-NPC inverter could feed the nonlinear load and also inject the remaining power into the grid with a unity PF and sinusoidal waveform. The harmonic filtering performance is tested for the active filtering function mode of the grid-connected PV system. The 3L-NPC inverter current harmonic spectrum is shown in Figure 16a in the only-PV system mode. Figures 16b and 16c show the grid current harmonic spectrum before and after shunt active filtering functionality of the PV system, respectively. The grid current THD values are reduced from 34.6% to 3.9%. These THD values of the 3L-NPC inverter currents are provided within the IEEE 519-1992 harmonic limits. According to the IEEE 519 standard, the total harmonic content of components transferred to the grid must be smaller than 5%.

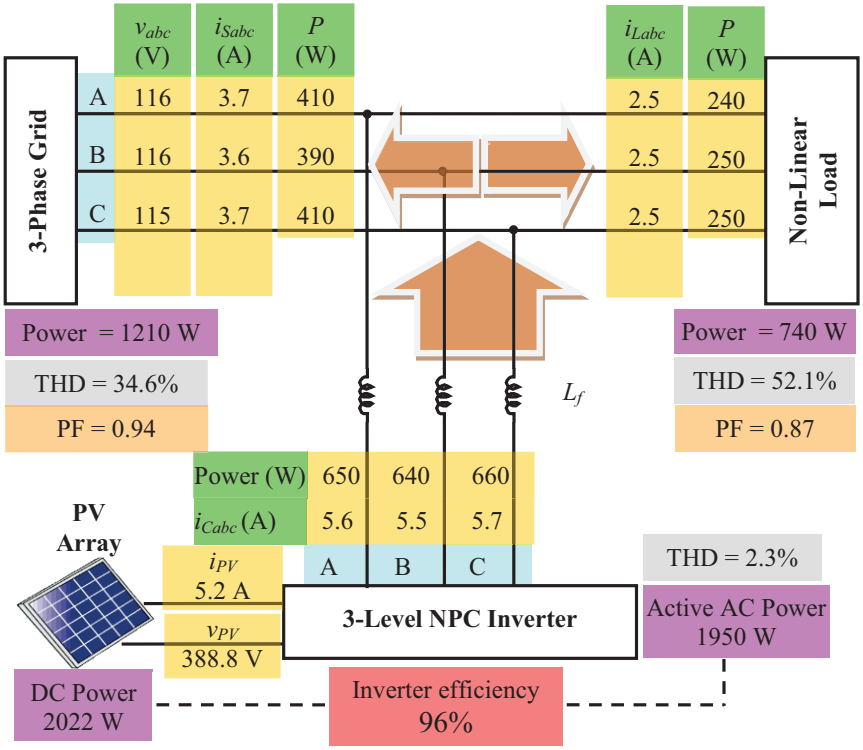

Figure 14. Electrical parameters of the PV system without shunt active filtering.

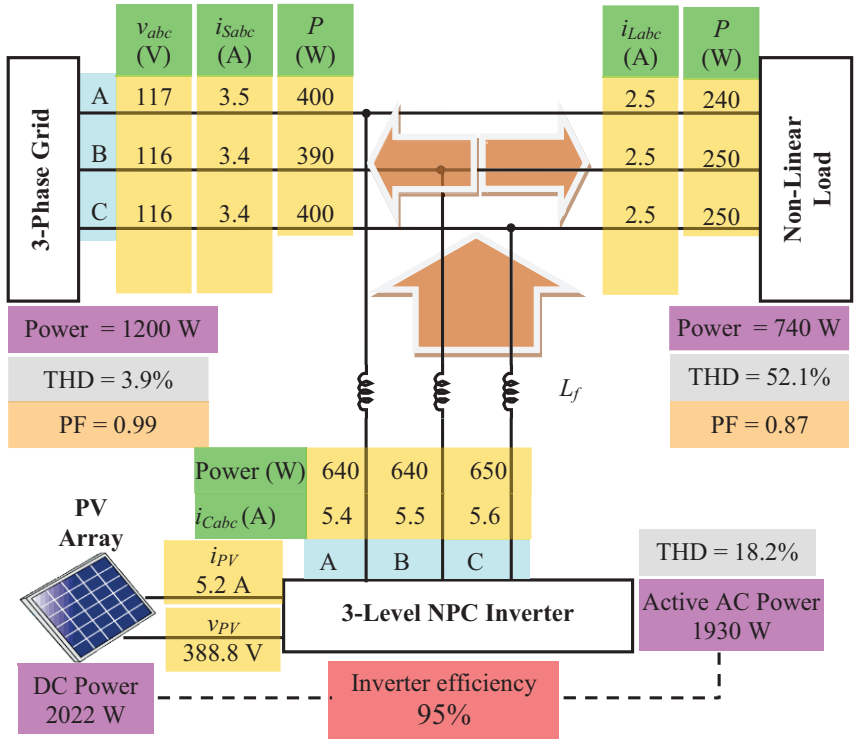

Figure 15. Electrical parameters of the PV system with shunt active filtering.

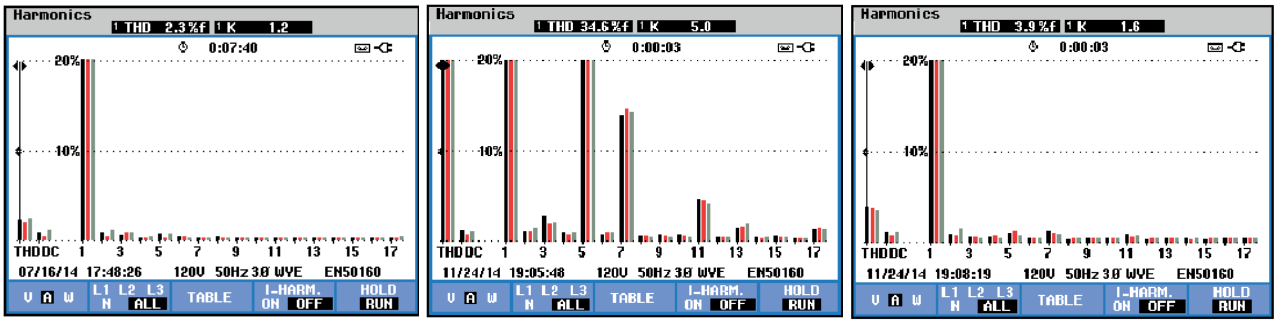

(a) (b) (c)

Figure 16. Harmonic spectrums of (a) 3L-NPC inverter currents with only PV system, (b) grid currents with only PV system, and (c) with PV system and shunt active filtering.

5. Conclusions

This paper presents the simulation and experimental performance of a single-stage three-phase 3L-NPC multilevel inverter-based multifunction PV power system with shunt active filtering capability. The proposed system can supply the maximum power from the PV system to the grid while filtering current harmonics and compensating reactive power caused by nonlinear loads. In the daytime with intensive irradiation, the three-phase solar PV power system provides active power together with active power filter functionality. At night and/or during no and/or poor irradiation times, the active power required by the loads is supplied from the mains while the PV system with 3L-NPC inverter provides harmonic filtering and PF correction. The performance of the proposed system has been confirmed by MATLAB/Simulink simulations and laboratory prototype experiments using the dSPACE DS1103 controller board. The experimental results show that the proposed multifunctional grid-connected PV power system is efficient for maximum PV power injection to the grid while filtering the load current harmonics and reactive power compensation together. The experimentally measured grid current THD results meet the IEEE 519-1992 harmonic restrictions and near-unity PF is achieved after compensation.

Acknowledgments

This research was supported by Kocaeli University BAP Project Number 2010/077. Thanks to Mr Halim Özmen from Semikron for experimental support.

References

[1] Teodorescu R, Liserre M, Rodriguez P. Grid Converters for Photovoltaic and Wind Power Systems. Hoboken, NJ, USA: Wiley-IEEE Press, 2011.

[2] Deutsche Gesellschaft für Sonnenenergie. Planning and Installing Photovoltaic Systems–A Guide for Installers, Architects and Engineers. 2nd ed. London, UK: Earthscan, 2008.

[3] Wang F, Duarte JL, Hendrix MAM. Grid-interfacing converter systems with enhanced voltage quality for microgrid application - concept and implementation. IEEE T Power Electr 2011; 26: 3501-3513.

[4] Abbasoglu S, Babatunde AA. Evaluation of field data and simulation results of a photovoltaic system in countries with high solar radiation. Turk J Elec Eng & Comp Sci 2015; 23: 1608-1618.

[5] Esram T, Chapman PL. Comparison of photovoltaic array maximum power point tracking techniques. IEEE T Energy Conver 2007; 22: 439-449.

[6] Brito MAG, Galotto L, Sampaio LP, Melo GA, Canesin CA. Evaluation of the main MPPT techniques for photovoltaic applications. IEEE T Ind Electron 2013; 60: 1156-1167.

[7] Subudhi B, Pradhan R. A comparative study on maximum power point tracking techniques for photovoltaic power systems. IEEE T Sustain Energ 2013; 4: 89-98.

[8] Bo Y, Wuhua L, Yi Z, Xiangning H. Design and analysis of a grid connected photovoltaic power system. IEEE T Power Electr 2010; 25: 992-1000.

[9] Tsang KM, Chan WL. Three-level grid-connected photovoltaic inverter with maximum power point tracking. Energ Convers Manage 2013; 65: 221-227.

[10] Sezen S, Ozdemir E. Modeling, simulation and control of three-phase three level multilevel inverter for grid connected photovoltaic system. J Optoelectron Adv M 2013; 15: 335-341.

[11] Ozdemir S, Altin N, Sefa I. Single stage three level grid interactive MPPT inverter for PV systems. Energ Convers Manage 2014; 80: 561-572.

[12] Colak I, Kabalci E, Bayindir R. Review of multilevel voltage source inverter topologies and control schemes. Energ Convers Manage 2011; 52: 1114-1128.

[13] Staudt I. Application Note AN-11001. 3L NPC & TNPC Topology. Nuremburg, Germany: Semrikon, 2012.

[14] Calleja H, Jimenez H. Performance of a grid connected PV system used as active filter. Energ Convers Manage 2004; 45: 2417-2428.

[15] Yu H, Pan J, Xiang A. A multi-function grid-connected PV system with reactive power compensation for the grid. Sol Energy 2005; 79: 101-106.

[16] Wu TF, Nien HS, Hsieh HM, Shen CL. PV power injection and active power filtering with amplitude-clamping and amplitude scaling algorithms. IEEE T Ind Appl 2007; 43: 731-741.

[17] Du CS, Zhang CH, Chen A. Amplitude limiting for the photovoltaic (PV) grid-connected inverter with the function of active power filter. In: IEEE 2010 2nd International Symposium on Power Electronics for Distributed Generation Systems; 16–18 June 2010; Hefei, China. New York, NY, USA: IEEE. pp. 426-432.

[18] Albuquerque FL, Moraes AJ, Guimaraes GC, Sanhueza SMR, Vaz AR. Photovoltaic solar system connected to the electric power grid operating as active power generator and reactive power compensator. Sol Energy 2010; 84: 1310-1317.

[19] Tsengenes G, Adamidis G. Investigation of the behavior of a three-phase grid-connected photovoltaic system to control active and reactive power. Electr Pow Syst Res 2011; 81: 177-184.

[20] Tsengenes G, Adamidis G. A multi-function grid connected PV system with three level NPC inverter and voltage oriented control. Sol Energy 2011; 85: 2595-2610.

[21] Marcos VM, Cadaval ER, Martinez MAG, Montero MIM. Three-phase single stage photovoltaic inverter with active filtering capabilities. In: IEEE 2012 38th Annual Conference on IEEE Industrial Electronics Society; 25–28 October 2012; Montreal, Canada. New York, NY, USA: IEEE. pp. 5253-5258.

[22] Noroozian R, Gharehpetian GB. An investigation on combined operation of active power filter with photovoltaic arrays. Int J Elec Power 2013; 46: 392-399.

[23] Zhou J, Liu M, Wei C, Gao C, Wu X. New three-dimensional space vector pulse width modulation of PV-AF system based on the ghγ coordinate system. Turk J Elec Eng & Comp Sci 2015; 23: 2017-2029.

[24] Martinez JA, Garcia JE, Arnaltes S. Direct power control of grid connected PV systems with three level NPC inverter. Sol Energy 2010; 84: 1175-1186.

[25] Suroso, Noguchi T. A new three-level current-source PWM inverter and its application for grid connected power conditioner. Energ Convers Manage 2011; 51: 1491-1499.

[26] Marei MI, Abdelaziz M, Assad AM. A simple adaptive control technique for shunt active power filter based on clamped-type multilevel inverters. Consumer Electronics Times 2013; 2: 85-95.

[27] Kale M, Özdemir E. A new hysteresis band current control technique for a shunt active filter. Turk J Elec Eng & Comp Sci 2015; 23: 654-665.

[28] Sezen S, Aktas A, Ucar M, Ozdemir E. A three-phase three-level NPC inverter based grid-connected photovoltaic system with active power filtering. In: IEEE 2014 16th International Power Electronics and Motion Control Conference and Exposition; 21–24 September 2014; Antalya, Turkey. New York, NY, USA: IEEE. pp. 1572-1576.

[29] Uçar M, Özdemir Ş, Özdemir E. A unified series-parallel active filter system for nonperiodic disturbance. Turk J Elec Eng & Comp Sci 2011; 19: 575-596.